Dynamics and kinetics of the astrochemical process C + $CH^+ \to C_2^+$ + H

Sergio Rampino

Scuola Normale Superiore
sergio.rampino@sns.it

Perugia, 7 June 2017

I. Introduction

I. Introduction
1. Overview

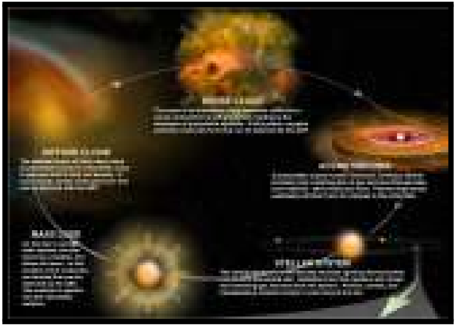

Star lifecycle

I. Introduction
1. Overview

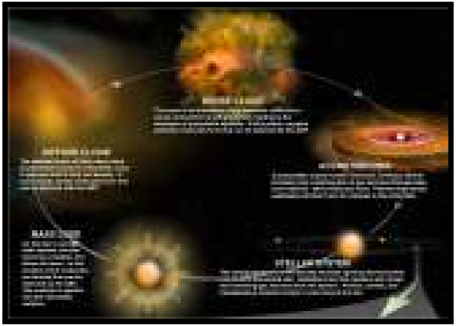

Star lifecycle

Molecular coulds:

low T (5-300 K)
low density (10^3-10^{14} cm^{-3})

I. Introduction

1. Overview

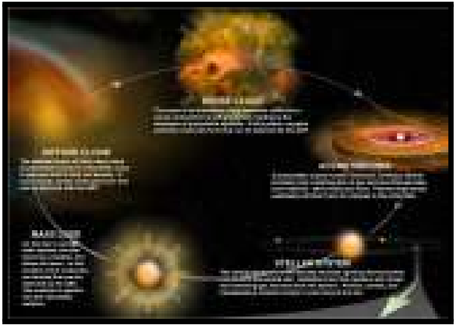

Star lifecycle

Molecular coulds:

low T (5-300 K)
low density (10^3-10^{14} cm^{-3})

What chemistry

Gas-phase barrierless reactions involving ions or radicals
Heterogeneous or multiphase processes involving dust grains and icy mantles

I. Introduction

1. Overview

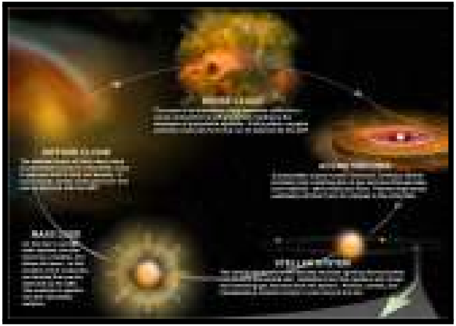

Motivation 1

Predicting the chemical evolution of the ISM helps in understanding star formation and in aging molecular clouds

What chemistry

Gas-phase barrierless reactions involving ions or radicals
Heterogeneous or multiphase processes involving dust grains and icy mantles

I. Introduction

1. Overview

Motivation 1

Predicting the chemical evolution of the ISM helps in understanding star formation and in aging molecular clouds

Motivation 2

The chemistry of the ISM might be at the basis of the origins of life on Earth (exogenous delivery)

I. Introduction

1. Overview

$$C + CH^+ \rightarrow C_2^+ + H$$

Motivation 1

Predicting the chemical evolution of the ISM helps in understanding star formation and in aging molecular clouds

Motivation 2

The chemistry of the ISM might be at the basis of the origins of life on Earth (exogenous delivery)

I. Introduction

1. Overview

Motivation 1

Predicting the chemical evolution of the ISM helps in understanding star formation and in aging molecular clouds

I. Introduction

2. Kinetic models

Processes

radiative association
associative detachment
dust-grain-catalysed reactions
photodissociation
colliaional dissociation
dissociative recombination
ion-neutral reactions
neutral-neutral reactions
charge-transfer reactions

I. Introduction

2. Kinetic models

Processes

radiative association
associative detachment
dust-grain-catalysed reactions
photodissociation
colliaional dissociation
dissociative recombination
ion-neutral reactions
neutral-neutral reactions
charge-transfer reactions

Model setup

number densities of all species (hundreds)
physical conditions within the cloud
set of reactions (thousands)
reactions rates for all chemical processes

I. Introduction

2. Kinetic models

Processes

radiative association
associative detachment
dust-grain-catalysed reactions
photodissociation
colliaional dissociation
dissociative recombination
ion-neutral reactions
neutral-neutral reactions
charge-transfer reactions

Model setup

number densities of all species (hundreds)
physical conditions within the cloud
set of reactions (thousands)
reactions rates for all chemical processes

Kinetic databases

KIDA
http://kida.obs.u-bordeaux1.fr/
UDfA
http://udfa.ajmarkwick.net/

I. Introduction

2. Kinetic models

Processes

radiative association
associative detachment
dust-grain-catalysed reactions
photodissociation
colliaional dissociation
dissociative recombination
ion-neutral reactions
neutral-neutral reactions
charge-transfer reactions

Many of the reactions in these databases need to be studied/revised

Model setup

number densities of all species (hundreds)
physical conditions within the cloud
set of reactions (thousands)
reactions rates for all chemical processes

Kinetic databases

KIDA
http://kida.obs.u-bordeaux1.fr/
UDfA
http://udfa.ajmarkwick.net/

I. Introduction

2. Kinetic models

Processes

radiative association
associative detachment
dust-grain-catalysed reactions
photodissociation
colliaional dissociation
dissociative recombination
ion-neutral reactions
neutral-neutral reactions
charge-transfer reactions

Many of the reactions in these databases need to be studied/revised

Model setup

number densities of all species (hundreds)
physical conditions within the cloud
set of reactions (thousands)
reactions rates for all chemical processes

Kinetic databases

KIDA
http://kida.obs.u-bordeaux1.fr/
UDfA
http://udfa.ajmarkwick.net/

I. Introduction

3. Ion-neutral reactions

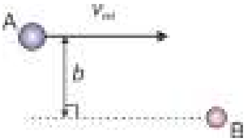

impact parameter

I. Introduction

3. Ion-neutral reactions

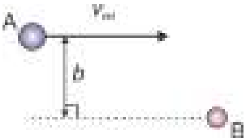

impact parameter

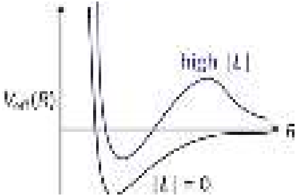

effective potential

I. Introduction

3. Ion-neutral reactions

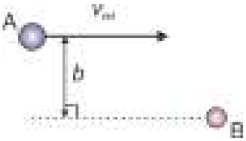

impact parameter

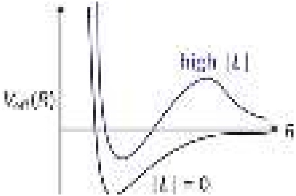

effective potential

Langevin capture model

the translational energy of reactants must only surpass a long-range centrifugal barrier for reaction to occur

I. Introduction

3. Ion-neutral reactions

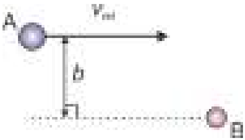

impact parameter

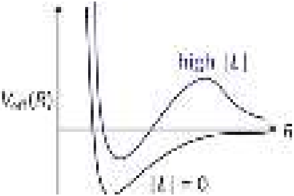

effective potential

Langevin capture model

the translational energy of reactants must only surpass a long-range centrifugal barrier for reaction to occur

Model rate coefficient

$$k = 2\pi e \sqrt{\frac{\alpha_{\mathrm{D}}}{\mu}}$$

(temperature independent)

I. Introduction
4. C + CH^+ reaction

lowest-energy reaction channel

$$C\,(^3P_0) + CH^+\,(X^1\Sigma^+) \rightarrow C_2^+\,(X^4\Sigma_g^-) + H\,(^2S_{1/2})$$

I. Introduction

4. C + CH^+ reaction

lowest-energy reaction channel

$$\mathrm{C}\ ({}^3P_0) + \mathrm{CH}^+\ (X^1\Sigma^+) \rightarrow \mathrm{C}_2^+\ (X^4\Sigma_g^-) + \mathrm{H}\ ({}^2S_{1/2})$$

CH^+
firstly detected
in the ISM in 1941

I. Introduction

4. C + CH^+ reaction

lowest-energy reaction channel

$$C\ (^3P_0) + CH^+\ (X^1\Sigma^+) \rightarrow C_2^+\ (X^4\Sigma_g^-) + H\ (^2S_{1/2})$$

CH^+
firstly detected
in the ISM in 1941

C_2^+
comtes Halley and
Jacobini-Zinner

I. Introduction
4. C + CH^+ reaction

lowest-energy reaction channel

$$C\ (^3P_0) + CH^+\ (X^1\Sigma^+) \rightarrow C_2^+\ (X^4\Sigma_g^-) + H\ (^2S_{1/2})$$

CH^+
firstly detected
in the ISM in 1941

C_2^+
comtes Halley and
Jacobini-Zinner

Model $k(T)$
1.2×10^{-9} cm^3 s^{-1}
(KIDA and UDfA)

I. Introduction
4. C + CH^+ reaction

lowest-energy reaction channel

$$\mathrm{C}\ ({}^3P_0) + \mathrm{CH}^+\ (X^1\Sigma^+) \rightarrow \mathrm{C}_2^+\ (X^4\Sigma_g^-) + \mathrm{H}\ ({}^2S_{1/2})$$

CH^+
firstly detected
in the ISM in 1941

C_2^+
comtes Halley and
Jacobini-Zinner

Model $k(T)$
1.2×10^{-9} cm^3 s^{-1}
(KIDA and UDfA)

Compare model versus dynamics $k(T)$

I. Introduction
4. C + CH^+ reaction

lowest-energy reaction channel

$$C\,(^3P_0) + CH^+\,(X^1\Sigma^+) \rightarrow C_2^+\,(X^4\Sigma_g^-) + H\,(^2S_{1/2})$$

CH^+
firstly detected
in the ISM in 1941

C_2^+
comtes Halley and
Jacobini-Zinner

Model $k(T)$
1.2×10^{-9} $cm^3\ s^{-1}$
(KIDA and UDfA)

Dynamics calculations

1. Sample configuration space
2. Compute a set of *ab initio* energies
3. Fit them with a functional form
4. Run the dynamics on the obtained PES
5. Work out observables

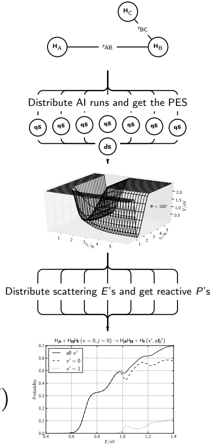

Compare model versus dynamics $k(T)$

II. PES

II. PES

5. SRBO

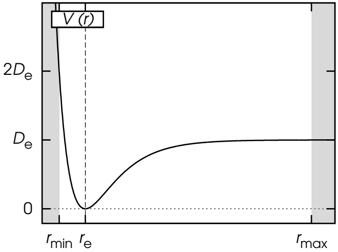

Configuration-space sampling

Conventional (BL) approach:

regular grid on r_1

regular grid on r_2

regular grid on ϕ

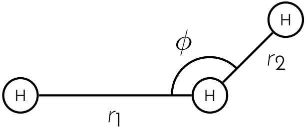

S Rampino, **Configuration-space sampling in potential energy surface fitting: a space-reduced bond-order grid approach**, *The Journal of Physical Chemistry A*, 2016, DOI: 10.1021/acs.jpca.5b10018

II. PES

5. SRBO

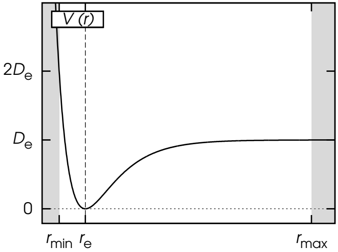

SRBO approach

switch from BL to BO space
introduce space-reduction param f

$$n = e^{-\beta(r - r_e)}$$

$$f = \frac{1 - n_{min}}{n_{max} - 1} = \frac{1 - e^{-\beta(r_{max} - r_e)}}{e^{-\beta(r_{min} - r_e)} - 1}$$

S Rampino, **Configuration-space sampling in potential energy surface fitting: a space-reduced bond-order grid approach**, *The Journal of Physical Chemistry A*, 2016, DOI: 10.1021/acs.jpca.5b10018

II. PES
5. SRBO

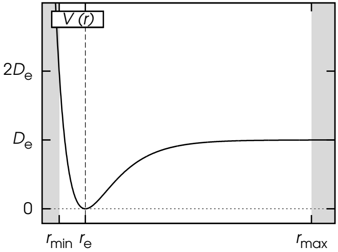

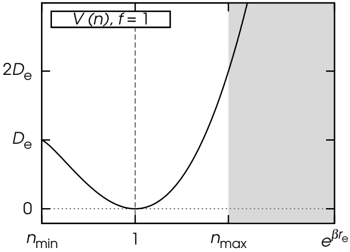

SRBO approach

switch from BL to BO space
introduce space-reduction param f

$$n = e^{-\beta(r - r_e)}$$

$$f = \frac{1 - n_{min}}{n_{max} - 1} = \frac{1 - e^{-\beta(r_{max} - r_e)}}{e^{-\beta(r_{min} - r_e)} - 1}$$

S Rampino, **Configuration-space sampling in potential energy surface fitting: a space-reduced bond-order grid approach**, *The Journal of Physical Chemistry A*, 2016, DOI: 10.1021/acs.jpca.5b10018

II. PES

5. SRBO

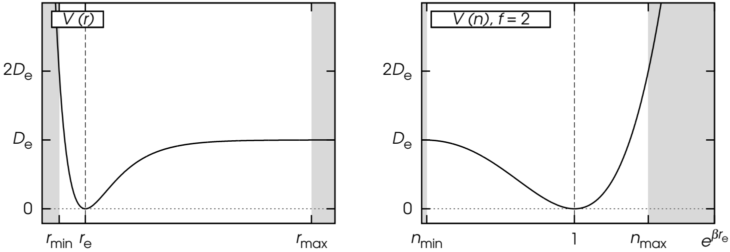

SRBO approach

switch from BL to BO space
introduce space-reduction param f

$$n = e^{-\beta(r - r_e)}$$

$$f = \frac{1 - n_{min}}{n_{max} - 1} = \frac{1 - e^{-\beta(r_{max} - r_e)}}{e^{-\beta(r_{min} - r_e)} - 1}$$

S Rampino, **Configuration-space sampling in potential energy surface fitting: a space-reduced bond-order grid approach**, *The Journal of Physical Chemistry A*, 2016, DOI: 10.1021/acs.jpca.5b10018

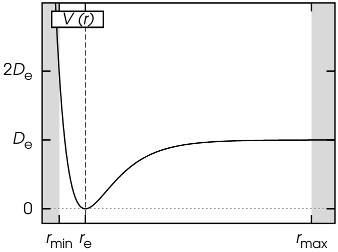

Configuration-space sampling

SRBO approach:

regular grid on n_1

regular grid on n_2

regular grid on ϕ

SRBO approach

switch from BL to BO space
introduce space-reduction param f

$$n = e^{-\beta(r - r_e)}$$

$$f = \frac{1 - n_{\text{min}}}{n_{\text{max}} - 1} = \frac{1 - e^{-\beta(r_{\text{max}} - r_e)}}{e^{-\beta(r_{\text{min}} - r_e)} - 1}$$

S Rampino, **Configuration-space sampling in potential energy surface fitting: a space-reduced bond-order grid approach**, *The Journal of Physical Chemistry A*, 2016, DOI: 10.1021/acs.jpca.5b10018

II. PES

5. SRBO

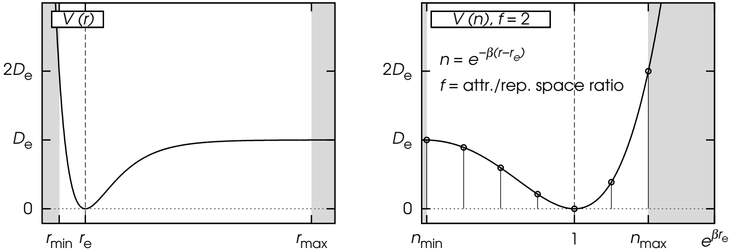

SRBO approach

switch from BL to BO space
introduce space-reduction param f

$$n = e^{-\beta(r-r_e)}$$

$$f = \frac{1-n_{\min}}{n_{\max}-1} = \frac{1-e^{-\beta(r_{\max}-r_e)}}{e^{-\beta(r_{\min}-r_e)}-1}$$

S Rampino, **Configuration-space sampling in potential energy surface fitting: a space-reduced bond-order grid approach**, *The Journal of Physical Chemistry A*, 2016, DOI: 10.1021/acs.jpca.5b10018

II. PES

5. SRBO

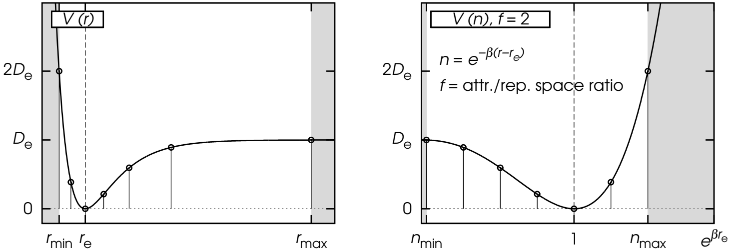

SRBO approach

switch from BL to BO space
introduce space-reduction param f

$$n = e^{-\beta(r-r_e)}$$

$$f = \frac{1-n_{\min}}{n_{\max}-1} = \frac{1-e^{-\beta(r_{\max}-r_e)}}{e^{-\beta(r_{\min}-r_e)}-1}$$

S Rampino, **Configuration-space sampling in potential energy surface fitting: a space-reduced bond-order grid approach**, *The Journal of Physical Chemistry A*, 2016, DOI: 10.1021/acs.jpca.5b10018

II. PES

5. SRBO

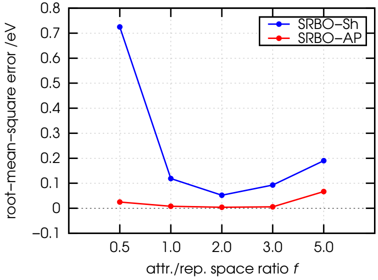

Best f, test on H_2

RMSE fit vs true diss. curve

$N = 13$

modified-Shepard interpolation

Aguado-Paniagua fitting

S Rampino, **Configuration-space sampling in potential energy surface fitting: a space-reduced bond-order grid approach**, *The Journal of Physical Chemistry A*, 2016, DOI: 10.1021/acs.jpca.5b10018

II. PES

5. SRBO

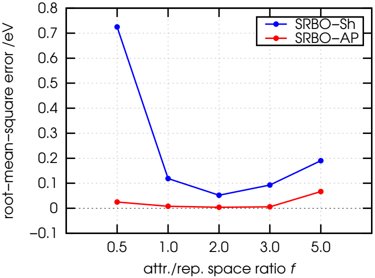

Best f, test on H_2

RMSE fit vs true diss. curve

$N = 13$

modified-Shepard interpolation

Aguado-Paniagua fitting

Optimal performances for $f = 2$

S Rampino, **Configuration-space sampling in potential energy surface fitting: a space-reduced bond-order grid approach**, *The Journal of Physical Chemistry A*, 2016, DOI: 10.1021/acs.jpca.5b10018

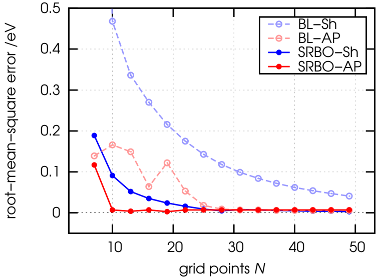

SRBO vs BL, test on H_2

RMSE fit vs true diss. curve

$f = 2$

modified-Shepard interpolation

Aguado-Paniagua fitting

S Rampino, **Configuration-space sampling in potential energy surface fitting: a space-reduced bond-order grid approach**, *The Journal of Physical Chemistry A*, 2016, DOI: 10.1021/acs.jpca.5b10018

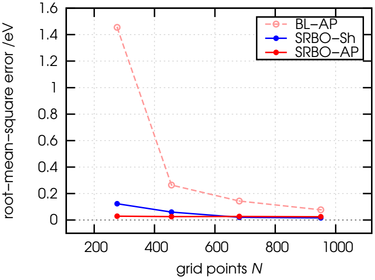

SRBO vs BL, test on H_3

RMSE fit vs true full 3D PES

$f = 2$

modified-Shepard interpolation

Aguado-Paniagua fitting

S Rampino, **Configuration-space sampling in potential energy surface fitting: a space-reduced bond-order grid approach**, *The Journal of Physical Chemistry A*, 2016, DOI: 10.1021/acs.jpca.5b10018

II. PES

5. SRBO

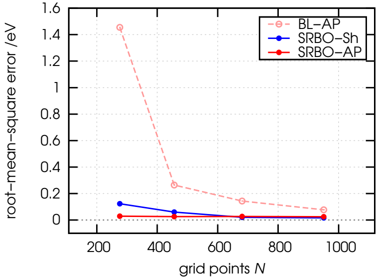

SRBO vs BL, test on H_3

RMSE fit vs true full 3D PES

$f = 2$

modified-Shepard interpolation

Aguado-Paniagua fitting

SRBO outperforms BL in converging the PES with increasing number of grid points

S Rampino, **Configuration-space sampling in potential energy surface fitting: a space-reduced bond-order grid approach**, *The Journal of Physical Chemistry A*, 2016, DOI: 10.1021/acs.jpca.5b10018

II. PES

6. Fitting

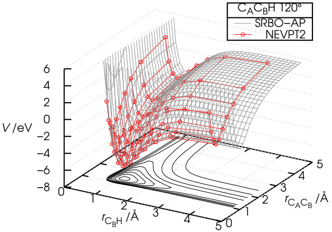

II. PES
6. Fitting

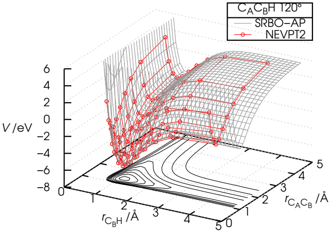

Configuration-space sampling

$f = 2$
10-point SRBO grids
5-point angular grid

II. PES

6. Fitting

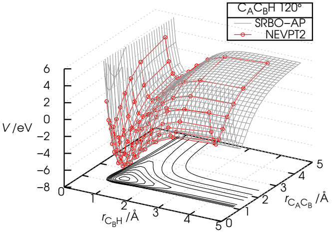

Configuration-space sampling

$f = 2$
10-point SRBO grids
5-point angular grid

Ab initio

PC-NEVPT2/CASSCF
DKH Hamiltonian
ANO-RCC basis set

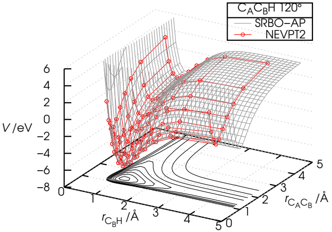

Configuration-space sampling

$f = 2$
10-point SRBO grids
5-point angular grid

Ab initio

PC-NEVPT2/CASSCF
DKH Hamiltonian
ANO-RCC basis set

Many-body expansion

$V(r_1, r_2, r_3) =$

$V_1^{(2)}(r_1) + V_2^{(2)}(r_2) + V_3^{(2)}(r_3)+$

$V^{(3)}(r_1, r_2, r_3)$

Fitting

775 *ab initio* energies
6th-degree polynomial fit for two-body terms
7th-degree polynomial fit for three-body term

A Aguado, M Paniagua, **A new functional form to obtain analytical potentials of triatomic molecules**, *The Journal of Chemical Physics* 96, 1265-1275 (1992)

II. PES

7. Channels

$C_A + C_BH^+ \rightarrow C_AC_B^+ + H$

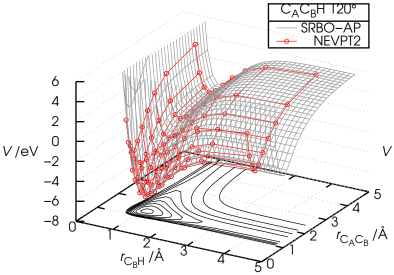

esoergic, favoured

$C_A + HC_B^+ \rightarrow C_AH^+ + C_B$

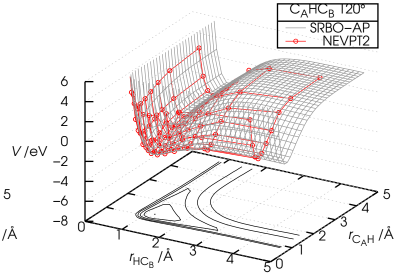

isoergic, less deep well

L Pacifici, M Pastore, E Garcia, A Laganà, S Rampino, **A dynamics investigation of the C + $CH^+ \rightarrow C_2^+$ + H reaction on an ab initio bond-order like potential**, *The Journal of Physical Chemistry A*, 2016, submitted

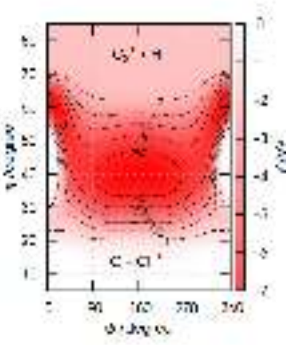

Rectangular relaxed plot

reaction coordinate
$\eta = \arctan\left(r_{CH}/r_{CC}\right)$

angular coordinate
$\Phi = \widehat{CCH}$

overall-size coordinate
$\rho = (r_{CH}^2 + r_{CC}^2)^{1/2}$

RRX plot
$\min_{\rho} V(\eta, \Phi)$

L Pacifici, M Pastore, E Garcia, A Laganà, S Rampino, **A dynamics investigation of the C + CH$^+ \rightarrow$ C$_2^+$ + H reaction on an ab initio bond-order like potential**, *The Journal of Physical Chemistry A*, 2016, submitted

II. PES

8. Reaction paths

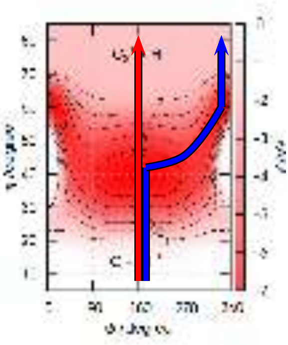

Reaction paths

path 1: collinear MEP

$C + CH^{+} \rightarrow CCH^{+} \rightarrow C_2^{+} + H$

path 2: absolute MEP

$C + CH^{+} \rightarrow CCH^{+} \rightarrow HCC^{+} \rightarrow H + C_2^{+}$

L Pacifici, M Pastore, E Garcia, A Laganà, S Rampino, **A dynamics investigation of the C + CH$^{+} \rightarrow$ C$_2^{+}$ + H reaction on an ab initio bond-order like potential**, *The Journal of Physical Chemistry A*, 2016, submitted

II. PES

8. Reaction paths

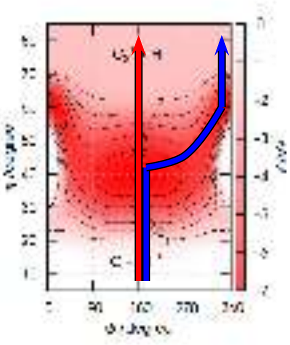

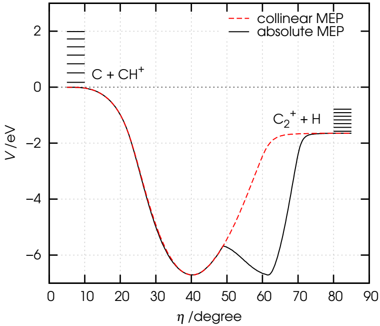

L Pacifici, M Pastore, E Garcia, A Laganà, S Rampino, **A dynamics investigation of the C + CH$^+$ → C$_2^+$ + H reaction on an ab initio bond-order like potential**, *The Journal of Physical Chemistry A*, 2016, submitted

II. PES

8. Reaction paths

Energetics

Exoergicity:
1.64 eV
1.73 eV (+ ZPE)

Well depth:
6.71 eV

Inter-well barrier:
1.04 eV

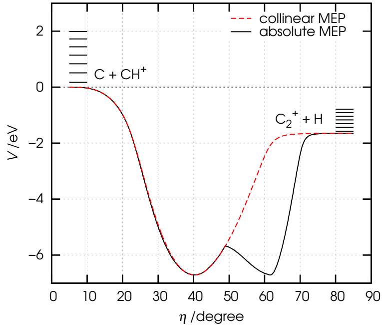

L Pacifici, M Pastore, E Garcia, A Laganà, S Rampino, **A dynamics investigation of the C + $CH^+ \rightarrow C_2^+$ + H reaction on an ab initio bond-order like potential**, *The Journal of Physical Chemistry A*, 2016, submitted

III. Dynamics

III. Dynamics
9. QCT vs QRS

QCT calculations

Program VENUS96

Trajectory

impact parameter b
collision energy E_{tr}
atom-diatom orientation angles
diatom's quantum-like internal states (v, j)

$N_{\mathrm{v,j}}(E_{\mathrm{tr}}, b)$: total trajectories
$N^{\mathrm{R}}_{\mathrm{v,j}}(E_{\mathrm{tr}}, b)$: reactive trajectories

III. Dynamics
9. QCT vs QRS

QCT calculations

Program VENUS96

Trajectory

impact parameter b
collision energy E_{tr}
atom-diatom orientation angles
diatom's quantum-like internal states (v, j)

$N_{v,j}(E_{tr}, b)$: total trajectories
$N^{R}_{v,j}(E_{tr}, b)$: reactive trajectories

Outcomes

opacity function

$$P_{v,j}(E_{tr}, b) = \frac{N^{R}_{v,j}(E_{tr}, b)}{N_{v,j}(E_{tr}, b)}$$

reactive probability

$$P_{v,j}(E_{tr}) = \frac{N^{R}_{v,j}(E_{tr})}{N_{v,j}(E_{tr})}$$

cross section

$$\sigma_{v,j} = \pi b^2_{max} \frac{N^{R}_{v,j}}{N_{v,j}}$$

thermal rate coefficient

$$k_{v,j}(T) = \langle v \rangle \sigma_{v,j} = \sqrt{\frac{8k_B T}{\pi\mu}} \pi b^2_{max} \frac{N^{R}_{v,j}}{N_{v,j}}$$

TD-QRS

Program RWAVEPR (D Skouteris)

III. Dynamics
9. QCT vs QRS

TD-QRS

Program RWAVEPR (D Skouteris)

1. set up a (v, j) wavepacket

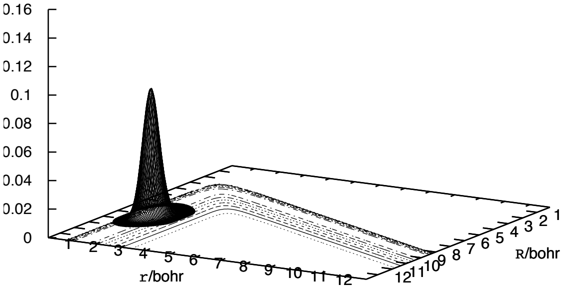

III. Dynamics
9. QCT vs QRS

TD-QRS

Program RWAVEPR (D Skouteris)

1. set up a (v, j) wavepacket
2. evolve in time

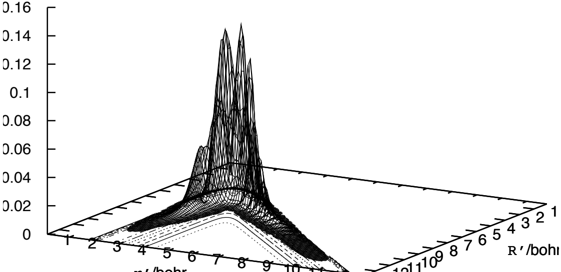

TD-QRS

Program RWAVEPR (D Skouteris)

1. set up a (v, j) wavepacket
2. evolve in time
3. analyse far into the product region

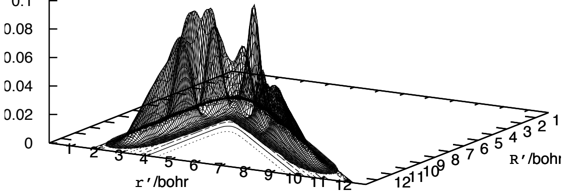

III. Dynamics
9. QCT vs QRS

TD-QRS

Program RWAVEPR (D Skouteris)

1. set up a (v, j) wavepacket
2. evolve in time
3. analyse far into the product region

80000 time iterations
400 $\times$ 400 (r', R') grid
GPU-based implementation

III. Dynamics

9. QCT vs QRS

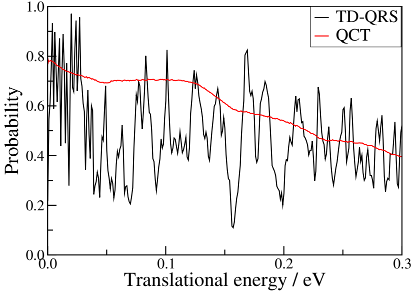

TD-QRS

Program RWAVEPR (D Skouteris)

1. set up a (v, j) wavepacket
2. evolve in time
3. analyse far into the product region

80000 time iterations
400×400 (r', R') grid
GPU-based implementation

state-specific ($v = 0$, $j = 0$) reactive probabilities

L Pacifici, M Pastore, E Garcia, A Laganà, S Rampino, **A dynamics investigation of the C + $CH^+ \rightarrow C_2^+$ + H reaction on an ab initio bond-order like potential**, *The Journal of Physical Chemistry A*, 2016, submitted

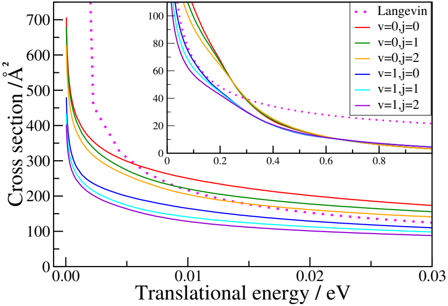

Reactive cross sections

L Pacifici, M Pastore, E Garcia, A Laganà, S Rampino, **A dynamics investigation of the C + $CH^+ \rightarrow C_2^+$ + H reaction on an ab initio bond-order like potential**, *The Journal of Physical Chemistry A*, 2016, submitted

III. Dynamics

10. Cross sections

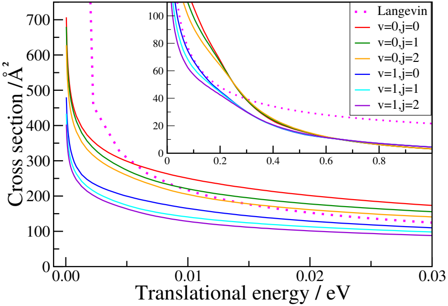

Reactive cross sections

diverge at vanishing E_{tr}

Langevin ok in 100-450 K

Langevin fails at low T

internal excitation lowers reactivity

L Pacifici, M Pastore, E Garcia, A Laganà, S Rampino, **A dynamics investigation of the C + $CH^+ \rightarrow C_2^+$ + H reaction on an ab initio bond-order like potential**, *The Journal of Physical Chemistry A*, 2016, submitted

III. Dynamics

11. Opacity functions

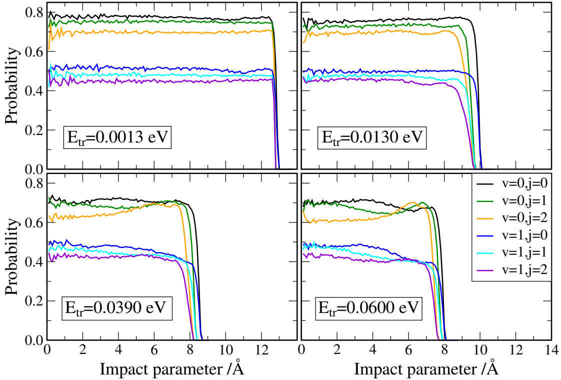

Opacity functions (10, 100, 300, 450 K)

L Pacifici, M Pastore, E Garcia, A Laganà, S Rampino, **A dynamics investigation of the C + CH$^+$ → C_2^+ + H reaction on an ab initio bond-order like potential**, *The Journal of Physical Chemistry A*, 2016, submitted

III. Dynamics

11. Opacity functions

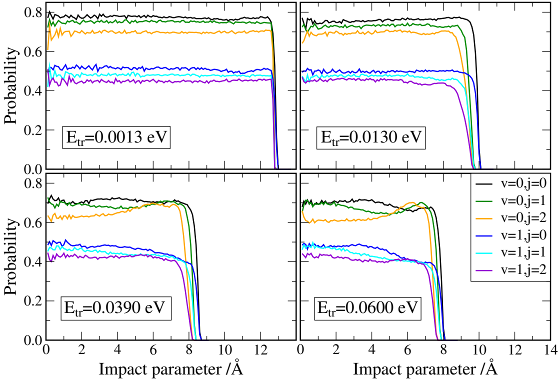

Opacity functions (10, 100, 300, 450 K)

capture-type mechanism at low collision energies

L Pacifici, M Pastore, E Garcia, A Laganà, S Rampino, **A dynamics investigation of the C + $CH^+ \rightarrow C_2^+$ + H reaction on an ab initio bond-order like potential**, *The Journal of Physical Chemistry A*, 2016, submitted

III. Dynamics

11. Opacity functions

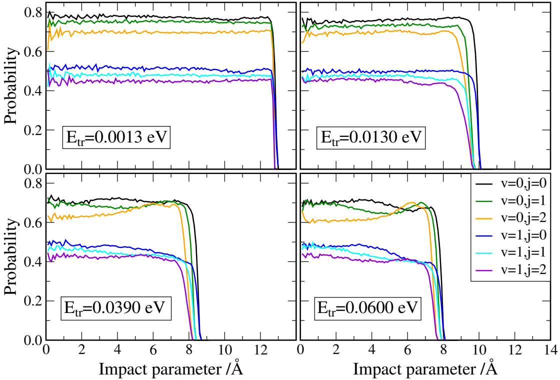

Opacity functions (10, 100, 300, 450 K)

capture-type mechanism at low collision energies
footprints of other mechanism showing up at higher collision energies

L Pacifici, M Pastore, E Garcia, A Laganà, S Rampino, **A dynamics investigation of the C + $CH^+ \rightarrow C_2^+$ + H reaction on an ab initio bond-order like potential**, *The Journal of Physical Chemistry A*, 2016, submitted

III. Dynamics

11. Opacity functions

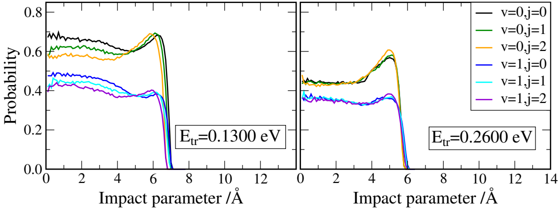

Opacity functions (1000, 2000 K)

capture-type mechanism at low collision energies
footprints of other mechanism showing up at higher collision energies

L Pacifici, M Pastore, E Garcia, A Laganà, S Rampino, **A dynamics investigation of the C + $CH^+ \to C_2^+$ + H reaction on an ab initio bond-order like potential**, *The Journal of Physical Chemistry A*, 2016, submitted

III. Dynamics

12. Product distributions

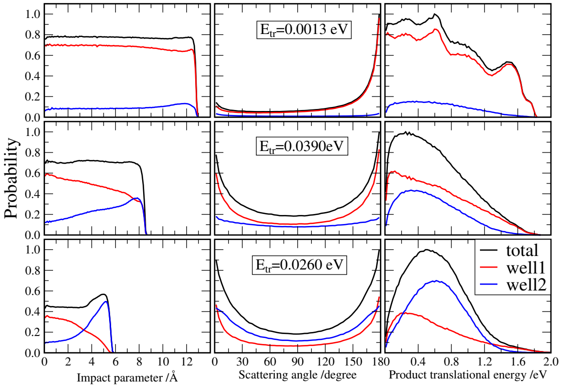

Opacity functions (10, 300, 2000 K)

capture-type mechanism at low collision energies
footprints of other mechanism showing up at higher collision energies

L Pacifici, M Pastore, E Garcia, A Laganà, S Rampino, **A dynamics investigation of the C + $CH^+ \to C_2^+$ + H reaction on an ab initio bond-order like potential**, *The Journal of Physical Chemistry A*, 2016, submitted

III. Dynamics
12. Product distributions

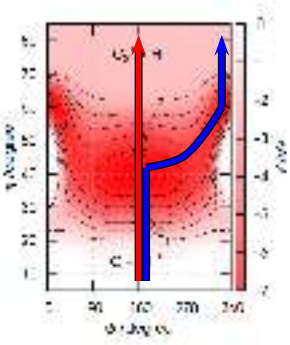

Reaction paths

path 1: collinear MEP

$C + CH^+ \rightarrow CCH^+ \rightarrow C_2^+ + H$

path 2: absolute MEP

$C + CH^+ \rightarrow CCH^+ \rightarrow HCC^+ \rightarrow H + C_2^+$

L Pacifici, M Pastore, E Garcia, A Laganà, S Rampino, **A dynamics investigation of the $C + CH^+ \rightarrow C_2^+ + H$ reaction on an ab initio bond-order like potential**, *The Journal of Physical Chemistry A*, 2016, submitted

III. Dynamics

12. Product distributions

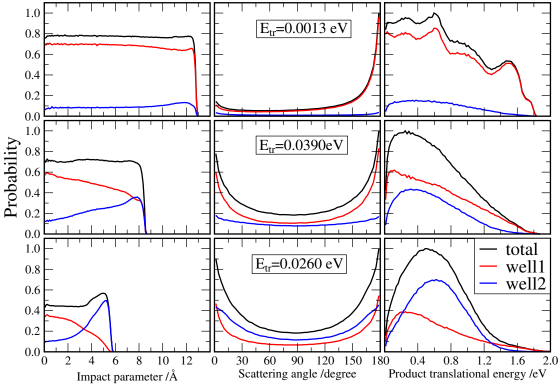

Opacity functions (10, 300, 2000 K)

capture-type mechanism at low collision energies
footprints of other mechanism showing up at higher collision energies

L Pacifici, M Pastore, E Garcia, A Laganà, S Rampino, **A dynamics investigation of the C + CH$^+$ $\rightarrow$ C$_2^+$ + H reaction on an ab initio bond-order like potential**, *The Journal of Physical Chemistry A*, 2016, submitted

IV. Kinetics

IV. Kinetics

13. Thermal $k(T)$

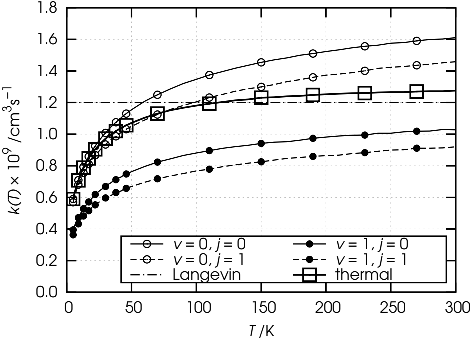

Model vs dynamics

S Rampino, M Pastore, E Garcia, L Pacifici, A Laganà, **On the temperature dependence of the rate coefficient of formation of C_2^+ from C + CH^+**, *Monthly Notices of the Royal Astronomical Society*, 2016, submitted

IV. Kinetics

13. Thermal $k(T)$

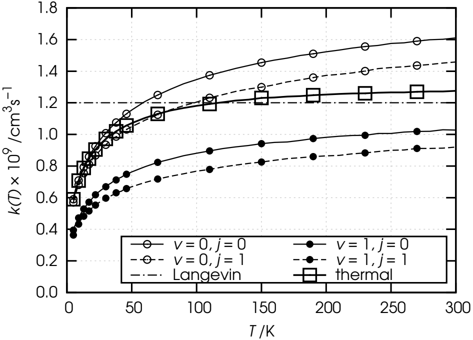

Model vs dynamics

factor two at low T

$k(T)$ doubles in 5-300 K

sharp increase in 5-50 K

S Rampino, M Pastore, E Garcia, L Pacifici, A Laganà, **On the temperature dependence of the rate coefficient of formation of C_2^+ from C + CH^+**, *Monthly Notices of the Royal Astronomical Society*, 2016, submitted

IV. Kinetics

13. Thermal $k(T)$

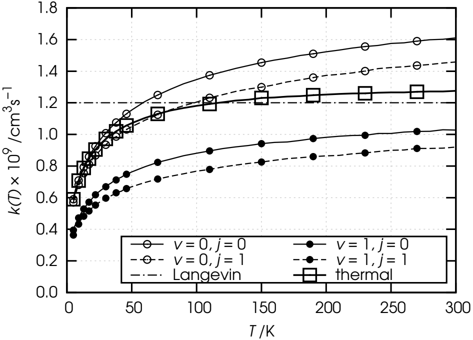

Model vs dynamics

factor two at low T

$k(T)$ doubles in 5-300 K

sharp increase in 5-50 K

Model calculations improperly enhance CH^+ consumption in kinetic models

S Rampino, M Pastore, E Garcia, L Pacifici, A Laganà, **On the temperature dependence of the rate coefficient of formation of C_2^+ from C + CH^+**, *Monthly Notices of the Royal Astronomical Society*, 2016, submitted

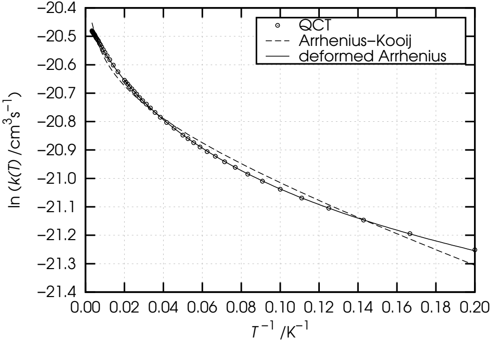

Fit formulæ

V Aquilanti, K C Mundim, M Elango, S Kleijn, T Kasai, **Temperature dependence of chemical and biophysical rate processes: phenomenological approach to deviations from Arrhenius law**, *Chemical Physics Letters* 498, 209-213 (2010)

IV. Kinetics

14. Fit

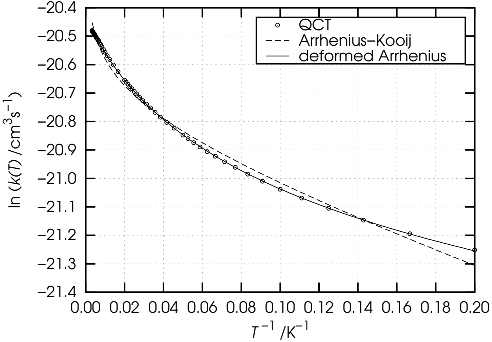

Fit formulæ

Arrhenius--Kooij:

$$k(T) = \alpha (T/300)^{\beta} e^{-\gamma/T}$$

deformed Arrhenius:

$$k(T) = A\left[1 - d\frac{\epsilon}{RT}\right]^{\frac{1}{d}}$$

V Aquilanti, K C Mundim, M Elango, S Kleijn, T Kasai, **Temperature dependence of chemical and biophysical rate processes: phenomenological approach to deviations from Arrhenius law**, *Chemical Physics Letters* 498, 209-213 (2010)

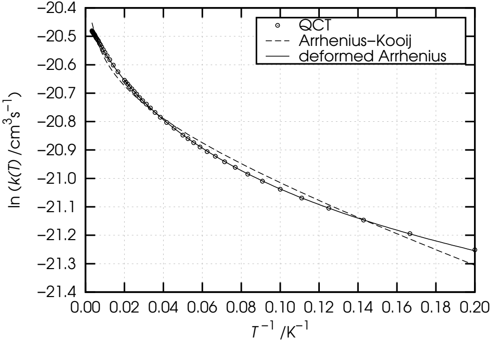

Fit formulæ

Arrhenius--Kooij:

$$k(T) = \alpha(T/300)^{\beta} e^{-\gamma/T}$$

deformed Arrhenius:

$$k(T) = A\left[1 - d\frac{\epsilon}{RT}\right]^{\frac{1}{d}}$$

Temperature dependence of $k(T)$ better conforms to the `deformed Arrhenius' law

V Aquilanti, K C Mundim, M Elango, S Kleijn, T Kasai, **Temperature dependence of chemical and biophysical rate processes: phenomenological approach to deviations from Arrhenius law**, *Chemical Physics Letters* 498, 209-213 (2010)

V. Conclusions

V. Conclusions

15. Summing up

Interaction

new bond-order based high-level *ab initio* PES
close inspection reveals alternative reaction paths

Dynamics

Langevin model fails at low T
competitive mechanisms (microscopic-branching) singled out

Kinetics

Langevin model at low T improperly enhances CH^+ destruction route
temperature dependence better conforms to the `deformed Arrhenius' law

Acknowledgments

Work done in collaboration with

Prof. Ernesto Garcia
Universidad del País Vasco, Vitoria (ES)

Dr. Mariachiara Pastore
CNRS, Nancy (FR)

Dr. Leonardo Pacifici
Università degli Studi di Perugia (IT)

Prof. Antonio Laganà
Università degli Studi di Perugia (IT)

Helpful discussions

Prof. Nadia Balucani
Università degli Studi di Perugia (IT)

Prof. Vincenzo Aquilanti
Università degli Studi di Perugia (IT)